European Journal of Phycology
March 2016, Volume 51, Issue 3, Pages 270-281
http://dx.doi.org/10.1080/09670262.2015.1134815
http://archimer.ifremer.fr/doc/00319/42990/

An emended description and phylogeny of the little-known *Prorocentrum sipadanense* Mohammad-Noor, Daugbjerg & Moestrup (Prorocentrales, Dinophyceae) from the Indian Ocean, Oman

Saburova Maria [1, *], Chomérat Nicolas [2]

[1] Environment and Life Sciences Research Center, Kuwait Institute for Scientific Research, P.O. Box 1638, 22017, Salmiya, Kuwait
[2] IFREMER, LER BO, Station de Biologie Marine, Place de la Croix, F-29900 Concarneau, France

* Corresponding author : Maria Saburova, email address : msaburova@gmail.com

Abstract :

A small *Prorocentrum* species was found during a pilot taxonomic survey of marine benthic dinoflagellates in the northwestern Arabian Sea, Oman. Based on the study of cells from natural samples and laboratory cultures using light and scanning electron microscopy, this taxon is attributed to the little-known *Prorocentrum sipadanense*, recorded so far only from East Malaysia. The description of this species has been emended to include details of internal cell structure, composition of its periflagellar area and intraspecific variability in size, shape and pore pattern. Round to oval or ovoid cells of *P. sipadanese* are surrounded by a prominent marginal ridge and are 17.9–23.9 µm long and 15.0–19.8 µm wide, with a foveate to reticulate thecal plate surface and asymmetric and scarce pore pattern. The small, V-shaped periflagellar area is composed of nine platelets. Cells possess two golden-brown chloroplasts with a central starch-sheathed pyrenoid and small posterior nucleus. In addition, the phylogenetic position of this taxon in *Prorocentrum* was revealed for the first time based on SSU and LSU rDNA data. The presence of *P. sipadanense* among epiphytic dinoflagellates from the Omani coast constitutes its first report from the Indian Ocean.

Keywords : Arabian Sea, benthic dinoflagellates, molecular phylogeny, morphology, Oman, *Prorocentrum sipadanense*, taxonomy

Introduction

Prorocentroid dinoflagellates are the most diverse group of thecate species occupying various benthic habitats mainly in sub-tropical and tropical areas, where are associated with sediments, macroalgae, mangroves, seagrasses and corals. Members of the genus *Prorocentrum* Ehrenberg have been shown to be an important integral part of the benthic dinoflagellate assemblages in shallow marine ecosystems worldwide (e.g., Faust, 1990; Marasigan *et al*., 2001; Faust *et al*., 2005; Mohammad-Noor *et al*., 2007; Saburova *et al*., 2009; Shah *et al*., 2013; Okolodkov *et al*., 2014). Over the last decades, benthic *Prorocentrum* species have been the subject of active research because of their potential toxicity with harmful effects on other marine organisms and human health (e.g., Faust & Gulledge, 2002 and references therein; Maranda *et al*., 2007).

To date, about thirty species of benthic *Prorocentrum* have been described, however, in some cases their taxonomy and phylogeny have been explored to a limited degree (Hoppenrath *et al*., 2013). In contrast to a few widely distributed and rather well studied species, including *P. lima* (Ehrenberg) Stein, *P. emarginatum* Fukuyo, *P. rhathymum* Loeblich III, Sherley et Schmidt, *P. concavum* Fukuyo, *P. belizeanum* Faust, and *P. hoffmannianum* Faust (e.g., Larsen & Nguyen, 2004; Faust *et al*., 2005; Mohammad-Noor *et al*., 2007; Herrera-Sepúlveda *et al*., 2015), many benthic *Prorocentrum* remain scarcely documented or only known from their original descriptions. Among these species, *P. sipadanense* Mohammad-Noor, Daugbjerg et Moestrup was originally described based on morphology of a few preserved cells isolated from the Malaysian coastal area (as *P. sipadanensis*, Mohammad-Noor *et al*., 2007). Because of limited material to a few cells and examination under a scanning

electron microscope only (N. Mohammad-Noor, pers. comm.), the morphology of internal cell structures including the shape of chloroplast, presence of pyrenoid and position of nucleus have been omitted in the diagnosis of *P. sipadanense*. Phylogenetic position of this species among other *Prorocentrum* is unknown because the sequence has yet to be obtained.

Recently, a minute *Prorocentrum* species was found during the pilot survey of benthic dinoflagellates along the Omani coast in the Arabian Sea, northern Indian Ocean. Based on its size, shape and characteristic pore pattern, it has been attributed to *P. sipadanense*. The diagnosis and description of *P. sipadanense* are emended herein to include the newly obtained details of its size range, morphological variability and internal structure of living cells on the basis of light and scanning electron microscopical observations. In addition, a molecular characterization has been performed to infer the phylogenetic position of *P. sipadanense* based on SSU and LSU rDNA data.

Materials and Methods

Sampling

Pilot taxonomical survey of the benthic dinoflagellate assemblages was performed at the Arabian Sea coast along Dhofar Governorate of the Sultanate of Oman at the end of winter monsoons in February 2014. The coastline of Dhofar is composed of extensive high cliffs alternating with shores of fine sands. For the Arabian Sea coast during the period of winter monsoons (December-February), the sea surface temperature typically

ranges from 23 to 28°C. Salinity of the surface waters is within range of 35.3-36.7 (e.g., Rixen *et al*., 2000).

Macroalgal thalli and surrounded sediments were collected in the vicinity of Salalah City at two sampling sites on the 24th and 25th of February 2014. The first sampling site was located to the westward of Salalah near Mirbat village at 16º58′03.8″N, 54º42′00.3″E in small semi-enclosed lagoon, where two macroalgal and five sediment samples were collected. The second site was located to the eastward of Salalah at 16º49′31.6″N, 53º42′14.1″E at open ocean shore, where six macroalgal and eight sediment samples were collected. Material was sampled in the upper subtidal zone from depths of 1.5-3 m during snorkeling by diver. Macroalgal thalli were sampled by hand; the upper layer of the bottom sediments was scraped to a depth 0.5-1 cm using 50 ml Falcon tubes. The water temperatures ranged between 26-27ºC during sampling.

Sample processing

Macroalgal thalli were shaken vigorously in plastic bottles with filtered seawater to detach epiphytic dinoflagellates. The samples were then passed through a 250 µm mesh sieve to remove large particles and then filtered on 20 µm mesh sieve to concentrate the dinoflagellate cells. The sand-dwelling dinoflagellates were separated from the sandy sediment by extraction using the frozen seawater method (Uhlig, 1964) with a 110 µm mesh size.

Isolation and culture maintenance

Cells of the small-sized *P. sipadanense* were observed sporadically in samples at low abundance. For this reason, culture studies of this species were carried out in order to increase the availability of material. Individual cells were isolated using sterilized capillary pipettes under an inverted microscope, washed at least 3 times in a drop of sterilized seawater, and then transferred to a 96-multiwell plate filled with 350 µl of sterile K medium without silicates (Keller *et al*., 1987) prepared with filter-sterilized (0.22 mm, Millipore) and autoclaved seawater. The isolated cells were incubated at 23.5°C under 80 µmol photons m^{-2} s^{-1} of light and 12:12 h light:dark photoperiod. When the cell concentration was sufficient, the contaminant-free isolate with dividing and motile cells was sub-cultured in 25 cm^2 tissue culture flasks containing 40 ml sterile K medium as stock culture (strain Om-P-sip-012).

Light and scanning electron microscopy

For detailed observation, cells from either mixed natural samples or cultures were isolated by micropipetting in preparation for high-magnification photomicroscopy, and were then examined at 630× to 1000× magnification with Leica DM2500 (Leica, Wetzlar, Germany) light microscope (LM) equipped with epifluorescence (100 W short arc mercury lamp), differential interference contrast (DIC) optics, and Leica DFC320 digital camera. LM observation of the thecal surface was performed on cells stained with Calcofluor White (Sigma Chemical Co.) according to the method of Fritz & Triemer (1985). Autofluorescence of the chloroplasts was generated using an excitation wavelength of 568 nm.

For scanning electron microscopy (SEM), concentrated cultures were preserved with Lugol-iodine solution to a final concentration of 4%. Fixed cells were sonicated and were then collected on a 5-µm polycarbonate membrane filter (Whatman Nucleopore Track-Etch), rinsed twice with deionized water and gradually dehydrated with increasing concentrations of ethanol (15, 30, 50, 70, 90, 95 and 100%). The filters were critical point dried, sputter-coated with gold-palladium and examined either by Tescan Vega-3 or by LEO Supra 50VP scanning electron microscopes with an electron acceleration of 5 kV. Alternatively, cells were prepared according to Chomérat & Couté (2008) and examined using a Quanta 200 (FEI, Eindhoven, the Netherlands) SEM. The SEM photographs were presented on a uniform background using Adobe Photoshop CS2, v. 9.0.2 (Adobe Systems, San Jose, CA, USA).

Morphometric measurements and nomenclature

Morphometric measurements were made either from the calibrated digital LM images using Leica Application Suite v. 3.7 software (Leica Microsystems Ltd, Switzerland) or were calculated from scanning electron micrographs. Cell dimensions were measured in two cells from the natural sample and in 30 cultured specimens. Dimensions are given as the mean ± standard deviation; n – number of measurements. Platelets of the periflagellar area were labeled following newly proposed nomenclature (Hoppenrath *et al*., 2013). The original species epithet '*sipadanensis*' was modified according to article 32.7 of the International Code of Botanical Nomenclature (McNeill *et al*., 2006) following Hoppenrath *et al*. (2013).

DNA amplification and sequencing

One to five cells from the culture were isolated with a micropipette under an inverted microscope (Olympus IX51, Tokyo, Japan), rinsed in drops of distilled water, and then placed into 0.2 mL PCR tubes containing about 3 µL of double-distilled water. The tubes were stored at -20°C until amplification. For PCR reaction, the tubes were thawed and the PCR Master Mix (Promega, Madison, WI, USA) and 25 pmol of each primer were added, as described previously in Nézan *et al*. (2012). The PCR products were purified using the Wizard SV Gel and PCR Clean-up system (Promega) according to the manufacturer's recommendations. Sequencing was realized using ABI PRISM Big Dye Terminator Cycle kit (Life Technologies, Carlsbad, CA, USA) and the purification kit Montage SEQ Sequencing Reaction Cleanup (Millipore, Billerica, MA, USA). The sequences were determined with an automated 3130 genetic analyzer (Applied Biosystems, Carlsbad, CA, USA).

Phylogenetic analyses

Phylogenetic analyses were realized separately for the small and large ribosomal DNA. For the SSU, the sequence of *P. sipadanense* was aligned together with 33 SSU sequences of other *Prorocentrum* species and 4 sequences of other dinoflagellates (as outgroup) retrieved from GenBank using the multiple sequences aligner SINA (Pruesse *et al*., 2012). The SSU data matrix comprised 38 SSU rDNA sequences and 1719 characters. For LSU, the sequence of *P. sipadanense* was aligned together with 31 LSU sequences of other *Prorocentrum* species and 2 sequences of *Scrippsiella* (as outgroup)

retrieved from GenBank using MAFFT software version 7 (Katoh & Standley, 2013), with selection of the Q-ins-I algorithm which considers the secondary structure for the alignment. The LSU data matrix comprised 34 LSU sequences and 955 characters. Both alignments were refined by eye.

The two data matrices were analyzed by two methods of phylogenetic reconstruction: maximum likelihood (ML), using PhyML v. 3.0 software (Guindon *et al*., 2010) and Bayesian inference (BI) using MrBayes v. 3.1.2 (Ronquist & Huelsenbeck, 2003). The software jModeltest v. 0.1.1 (Posada, 2008) was first used to select the most suitable model of substitutions. For both matrices, a General Time Reversible model with invariant sites and a gamma correction for among-site rate variation was chosen (GTR + I + Γ). Bootstrap values (support for branches) of trees were obtained after 1000 iterations in ML. For Bayesian inference, four Markov chains were run simultaneously for 2×10^6 generations with sampling every 100 generations. On the 2×10^4 trees obtained, the first 2000 were discarded (burn-in) and a consensus tree was constructed from the remaining trees. The posterior probabilities corresponding to the frequency with which a node is present in preserved trees, were calculated using a coupled Monte Carlo Metropolis approach – Markov Chain (MCMC).

Results

During the course of our pilot taxonomic survey on the benthic dinoflagellates assemblage in the coastal area of the Sultanate of Oman, we found a small *Prorocentrum* species that highly resembles *P. sipadanense*, a species known so far only from the shore of the Sipadan Island in the western Pacific Ocean, East Malaysia

(Mohammad-Noor *et al*., 2007). Among the studied Omani benthic dinoflagellates, this small *Prorocentrum* occurred in low abundance, and several cells have been isolated to establish a culture for comprehensive investigation of its morphology, intraspecific variability and phylogeny. In this study, we observed morphological characters for cultured cells as well as a few specimens from natural sample were included into analysis. To clarify the identity of this *Prorocentrum*, cells were examined in detail using light and scanning electron microscopy, which resulted in the emended description herein.

Taxonomic description

***Prorocentrum sipadanense* Mohammad-Noor, Daugbjerg et Moestrup emend. Saburova et Chomérat (Figs 1-30)**

Emended diagnosis: Cells round to oval or ovoid, with asymmetric oblique truncated apex and prominent flat marginal ridge, 17.9-23.9 µm long and 15.0-19.8 µm wide (the lowest range noted in Mohammad-Noor *et al*., 2007) in lateral thecal plate view. ~~Valve~~Thecal plate surface foveate to reticulate with characteristic asymmetric and scarce pore pattern (a few closely spaced paired pores or seldom triplets and single pores). Plate centre devoid of pores. Irregular row of marginal pores. Pores round, inside depressions, with diameter of 0.11-0.17 µm. Periflagellar area small, wide V-shaped, composed of nine platelets (1 2 3 4 5 6a,b 7 8). Platelets 1, 2 and 5 with depressions. Flagellar pore large, oval. Accessory pore much smaller. Intercalary band smooth. Two

golden-brown chloroplasts with central pyrenoid, surrounded by starch ring along each lateral cell side. Small round to oval nucleus located posterior. Epiphytic on macroalgae.

Epitype: SEM stub of strain Om-P-sip-012 is designated here as epitype for *P. sipadanense* Mohammad-Noor, Daugbjerg et Moestrup emend. Saburova et Chomérat (Figs 21-23, 25, 27). It is deposited at the CEDiT (Centre of Excellence for Dinophyte Taxonomy) dinoflagellate type collection, Wilhelmshaven, Germany (identification number CEDiT2015E50).

Additional strain materials: Living cultures of strain Om-P-sip-012 are deposited at the Culture Collection of Kuwait Institute for Scientific Research (Kuwait). Lugol-preserved cells of strain Om-P-sip-012 were deposited in the Centre of Excellence for Dinophyte Taxonomy, Wilhelmshaven, Germany (identification number CEDiT2015RM51). Sequences # KT308151 and # KT308152 were obtained from this culture and deposited in GenBank.

Emended species description: Cells are small, 17.9-23.9 µm long (mean 21.90 ± 1.22, n=29), 15.7-19.8 µm wide (mean 18.16 ± 0.87, n=26) in ~~valve~~lateral thecal plate view (depth), and 7.3-9.3 µm thick (mean 8.51 ± 0.68, n=6; ~~measured as the length of the dorso-ventral axis~~width in intercalary band view), with the length to width ratio varying from 1.13 to 1.45 (mean 1.22 ± 0.06, n = 24). Cell shape is oval to ovoid, with asymmetrical oblique truncated apex (Figs 1-6, 14, 17, 21, 25). In right thecal view, the dorsal edge of apex appears to be roundly truncated and lower than the slightly pointed ventral edge (Figs 1-4, 14, 17, 21). The antapex is widely rounded. Right thecal plate is

nearly flat at the centere and gradually rounded toward the margins (Figs 13, 21-23), whereas left thecal plate is slightly concave in its centere (Figs 22, 27). The thecal plate margins form a prominent flat ridge that appears as a flange surrounding the cell (Figs 2, 3, 6, 9-13, 14). Cell possesses two golden-brown deeply lobed to reticulate chloroplasts lying along each lateral cell side. Each chloroplast is associated with a centrally located pyrenoid, surrounded by a starch ring (Figs 2, 3, 5, 6-8, 10). Nucleus is small, round and posteriorly located (Figs 3, 4, 6, 11).

Thecal plate surface is foveate to somewhere reticulate, and is ornamented with small, shallow and closely appressed depressions (Figs 12, 13, 15, 18, 21-27). Depressions are round or oval to polygonal with diameter ranging between 0.24-0.75 µm, n=10 (Figs 21-27). Small round pores with diameter 0.11-0.18 µm (0.14 ± 0.02, n=17) are located inside some depressions and arranged in distinct scarce and asymmetrical pore pattern. A few closely spaced pairs or seldom triplets and single pores are asymmetrically scattered on the thecal surface, but the centere of both thecal plates is devoid of pores (Figs 12, 15-17, 21, 26). The pores in group are mostly arranged in adjacent depressions, but can be located more distant from each other (Figs 21, 26). There are 20-26 pores on each thecal plate. Unequally spaced marginal pores run alongside the periphery of thecal plates (Figs 12, 13, 17, 18, 21, 26). There are 39-47 marginal pores along each thecal plate margin (n=7). The thecal plate margins are bordered by the row of depressions without pores at their bottom. The adjacent marginal ridge is wide and smooth (Figs 13, 17, 18, 21-23, 26).

The periflagellar area is small, wide V-shaped and located in apical indention of the right thecal plate (Figs 2, 14, 17, 19, 20, 21-24). It is composed of nine small platelets, namely, 1, 2, 3, 4, 5, 6a, 6b, 7 and 8 (Fig. 20). The flagellar pore is large, oval

and surrounded by four platelets including 3, 5, 6a and 8. Accessory pore is much smaller, almost circular and surrounded by the platelets 2, 8, 6b and 7. The platelet 5 is in contact with 3, 4 and 6a but is distant from platelet 8. The platelets 1, 2 and 5 are ornamented with a few depressions. All the platelets have raised borders but no platelet lists, wings or protrusions were determined from our observations (Figs 19, 20, 22-24).

Behavior in culture: In culture during the growing phase, cells of *P. sipadanense* were mostly attached to the bottom, often forming a more or less long chains of dividing cells within a mucilage envelop similar to those observed in *P. levis* Faust, Kibler, Vandersea, Tester & Litaker (Faust *et al*., 2008). In the stationary phase, most of the cells were observed in the motile form. On the contrary, in old cultures, the nonmotile cells were prevailed. In this stage, cell size started to reduce gradually due to successive shedding of thecae with ageing of culture in response to nutrient depletion. These small-sized cells were observed to be embedded in chains of their nested half-open empty thecae (Figs 28-30). Such cells appeared to be more rounded and smaller than motile cells (Fig. 28). Being inoculated into fresh medium, small nonmotile cells left the chains of their empty thecae, began to swim, increased in size and started to divide.

Epitype locality: The strain Om-P-sip-012 was isolated from the epiphytic assemblage on *Padina* sp. collected from the upper subtidal zone in the vicinity of Salalah City (Omani coast in the Arabian Sea, northern Indian Ocean at 16º58′03.8″N, 54º42′00.3″E) on 24.02.2014 by M. Saburova.

Distribution: During this study, the taxon identified here as *P. sipadanense* was found epiphytically on *Padina* sp. collected in subtidal zone of the Arabian Sea coast in Oman in the vicinity of Salalah City. This small *Prorocentrum* species occurred rarely and represented a relatively low proportion of the overall epiphytic dinoflagellate assemblage.

Phylogenetic position

Both phylogenies inferred from SSU and LSU showed that the sequences of *P. sipadanense* are not closely related to any other *Prorocentrum* sequences available. In the SSU tree (Fig. 31), this species forms a new branch basal to the clade comprising most of symmetric and benthic species but with a low support. In the LSU tree, *P. sipadanense* clusters with *P. borbonicum* Ten-Hage, Turquet, Quod, Puiseux-Dao & A. Couté, another small benthic *Prorocentrum* species, with a strong posterior probability in BI but only a moderate support in ML (Fig. 32). The position of the clade formed by these two species is however not supported and it cannot be confirmed that it is related to symmetric/benthic species from the LSU phylogeny.

Discussion

The original description and illustrations of *Prorocentrum sipadanense* were based solely on a SEM observation of two preserved cells (Mohammad-Noor *et al*., 2007; Hoppenrath *et al*., 2013; N. Mohammad-Noor pers. comm.), and therefore were focused on the cell size, shape and thecal surface, with lacking details on cytoplasm content.

This taxon was characterized by a small size (18-19 µm long and 15-16 µm wide), round to ovate cell shape, heavily ornamented theca with distinct pore pattern and presence of marginal pores (Mohammad-Noor *et al*., 2007). Since its discovery, the species was considered as rare and little-known due to its scarce description and lack of further trustworthy records (Hoppenrath *et al*., 2013).

In this paper we present a detailed reinvestigation of a taxon, which we interpreted as conspecific with that described by Mohammad-Noor *et al*. (2007) as *P. sipadanense*. Our new observations added previously unreported details to the original description of this species regarding the cell shape, asymmetry of the apical end, the structure of the periflagellar area, the thecal surface ornamentation and pore sizes, the presence and shape of the chloroplasts and pyrenoids, and the nucleus localization based on observations of alive and preserved cells by LM and SEM. The greater number of specimens examined allowed us to document variability in cell shape and size, and in thecal surface ornamentation. Furthermore, the phylogenetic position of *P. sipadanense* among the other *Prorocentrum* species has been revealed for the first time based on the molecular analyses of the established cultures.

The main characters for species discrimination within the genus *Prorocentrum* are based on cell shape and size, thecal surface and intercalary band morphology, and structure of the periflagellar area. Among the *Prorocentrum* species, the presence or absence and organization of pyrenoids are given taxonomic importance (e.g., Hoppenrath *et al*., 2013).

The taxon reinvestigated here corresponds well with the original description of *P. sipadanense* (Mohammad-Noor *et al*., 2007) in respect of its small size and characteristic pore pattern, although it differs in details of cell shape and thecal plates

asymmetry. Based on our observations on the motile cells, their shape was shown to be rather ovoid than round to oval as originally stated. Additionally, the cell apex was shown to have slight but distinct asymmetry with lower and roundly truncated dorsal edge versus pointed and higher ventral edge that can be considered as a diagnostic character for this species. One more noticeable feature of the cell morphology in our material was the presence of a distinct smooth ridge around the cell margins. Marginal ridge is clearly distinguished from the published SEM images of the holotype (Fig. 12 a, b in Mohammad-Noor *et al*., 2007), however this character has been omitted in the original description of *P. sipadanense*.

Although traditionally the shape and size of ~~valve~~cell are considered among the main morphological criteria in taxonomy of *Prorocentrum*, it has been shown recently that these features can be the subject to a high variability in some *Prorocentrum* species (e.g., Nagahama *et al*., 2011; Hoppenrath *et al*., 2013). Revealed distinctions in the cell shape and asymmetry in *P. sipadanense* from Oman compared to the type material can be interpreted by intraspecific variability in this species. Actually, some slight asymmetry in the apex is discernible from the provided SEM images of the holotype specimen (Fig. 12a in Mohammad-Noor *et al*., 2007). In the current observations, this species appeared to be morphologically variable. In senescent cultures, two different morphotypes corresponding either to larger and asymmetrical motile cells or smaller and rounded nonmotile specimens were observed (Fig. 28).

One more difference of our material compared with holotype of *P. sipadanense* concern the thecal surface ornamentation when it was viewed by SEM. As visible in the provided SEM images of type material (Fig. 12 in Mohammad-Noor *et al*., 2007), on the thecal surface of *P. sipadanense* the depressions possessing pores are deeper

compared with surrounded depressions without pores, whereas no difference in depressions with or without pores was observed in our material. We suppose that this discrepancy between images provided in the original description of *P. sipadanense* and those obtained from our material can be considered as an artifact in the preparation for SEM. Probably, the thecal surface of the type material looks more raised in SEM images due to a very thin unremoved mucilage layer or outer membranes.

The pore pattern on the thecal surface is traditionally considered as one of the most important taxonomic character in the genus *Prorocentrum* (e.g., Steidinger & Tangen, 1996; Faust *et al*., 1999; Hoppenrath *et al*., 2013). The pore pattern of *P. sipadanense* has been shown to be composed of scarce and asymmetrically scattered ~~valve~~ pores except the ~~cell~~ centre of thecal plates and uneven row of marginal pores (Mohammad-Noor *et al*., 2007). This combination is unique among the existing *Prorocentrum* species. Given this characteristic pore pattern, our material can be attributed to *P. sipadanense*. Some observed variability in the number of pores in the Omani specimens in comparison with type material (Table 1) may be caused by differences in cell size or age.

Relatively small periflagellar area is commonly the most complicated issue in taxonomy of *Prorocentrum*, however, the structure of this area including the number, shape and composition of small platelets is an important taxonomic character (e.g., Faust *et al*., 1999; Hoppenrath *et al*., 2013). As originally described and subsequently interpreted, wide V-shaped periflagellar area of *P. sipadanense* possesses large flagellar and smaller accessory pores surrounded by eight platelets (Mohammad-Noor *et al*., 2007; Hoppenrath *et al*., 2013). Moreover, the composition of periflagellar area in *P. sipadanense* was previously considered as exception to the typical structure of the

periflagellar area in *Prorocentrum*, in which the fifth platelet never to be in contact with eighth (Hoppenrath *et al*., 2013). Based on detailed observation of the periflagellar area in Omani strain of *P. sipadanense* by LM (epifluorescence) and SEM, nine platelets (1 2 3 4 5 6a,b 7 8) were discerned in the present study for the first time. Additionally, similarly to other *Prorocentrum* species the fifth platelet was found to be dislocated from eighth but was connected with 3, 4 and 6a.

During morphological observations on the living cells of *P. sipadanense* in this study, some new features of ~~its~~their internal morphology were observed such as the presence of two chloroplasts associated with centrally located pyrenoids surrounded by starch sheath as well as posterior position of nucleus was shown. In some cells, anterior pusule was observed. The revealed internal structure of Omani strain of *P. sipadanense* can be considered as the typical for most benthic *Prorocentrum*.

Most of the benthic *Prorocentrum* species vary in size from 30 to 55 µm, and only a few species are much smaller including *P. borbonicum*, *P. elegans* Faust, *P. formosum* Faust, *P. norrisianum* Faust et Morton, and *P. sipadanense* (Hoppenrath *et al*., 2013). Probably because of their small sizes, these species may have been overlooked or misidentified during the most of taxonomic surveys on benthic dinoflagellates worldwide; therefore, the small-sized *Prorocentrum* species are rarely recorded and scarce documented in literature.

Among the small-sized species, *P. sipadanense* and *P. borbonicum* are the most morphologically similar to each other in terms of the cell size and the ornamentation of thecal surface (Table 1), whereas both of them are easily distinguished from other small benthic *Prorocentrum* with smooth thecal surface (Ten-Hage *et al*., 2000; Mohammad-Noor *et al*., 2007). The features, on which *P. sipadanense* can be reliably distinguished

from morphologically similar *P. borbonicum* is the pore pattern. Despite the small size of cell, distinct scarce and asymmetrically scattered thecal pores in combination with marginal pores are quite clearly visible in cells of *P. sipadanense* even by LM, whereas the unusual presence of tiny pores in ~~valve~~the cent~~e~~re of thecal plates as well as the occurrence of ~~valve~~thecal pores inside and between depressions in *P. borbonicum* can be revealed only by SEM (Ten-Hage *et al*., 2000; Hoppenrath *et al.*, 2014). Moreover, *P. sipadanense* and *P. borbonicum* are related species in the phylogenetic analysis inferred from LSU rDNA, which is consistent with the results obtained with morphology. However, the branch lengths indicated that their sequences are rather divergent and this argues in favor of two different species. This information cannot be confirmed in the SSU analysis since no sequence is yet available for *P. borbonicum*.

In performed phylogenetic analyses, *P. sipadanense* is related to species potentially known as toxic. In the SSU rDNA phylogeny, it is basal to the clade of benthic *Prorocentrum* species of which several are known to produce DSP toxins, including *P. hoffmannianum*, *P. lima*, *P. concavum*, *P. faustiae* Morton, and *P. maculosum* Faust (e.g., Faust & Gulledge, 2002; Moestrup *et al*., 2015). In the LSU rDNA phylogeny, *P. sipadanense* groups with *P. borbonicum* isolated from Réunion Island, which has been shown to be a producer of neurotoxic compounds that exhibited palytoxin-like effects (Ten-Hage *et al*., 2000, 2002). Later the toxicity of *P. borbonicum* has been confirmed in strain isolated from the Mediterranean Sea (Aligizaki *et al*., 2009). Based on the revealed phylogenetic relationships of *P. sipadanense*, this species could be considered as potential phycotoxin producer; however, further studies to confirm this hypothesis are required.

The known distribution of *P. sipadanense* is clearly limited on a global basis. Until now, this species has only been known from its type locality in East Malaysia, in the Celebes Sea of the western Pacific Ocean (Mohammad-Noor *et al*., 2007). Recent records of small benthic *Prorocentrum* resembling *P. sipadanense* in size and shape from the northern coast of the Yucatan Peninsula, the Gulf of Mexico, North Atlantic Ocean (Okolodkov *et al*., 2014, as *P*. cf. *sipadanensis*) and from the Jordanian coast of the Gulf of Aqaba in northern Red Sea (unpublished data of the first author) need to be confirmed by further morphological and phylogenetic studies. In the current study, *P. sipadanense* was found among benthic dinoflagellate assemblage from the coast of Oman in the northwestern Arabian Sea, Indian Ocean. This is the first report o~~n~~f this species after that of Mohammad-Noor *et al*. (2007) and the first report to deposit its sequence in GenBank. The observations of *P. sipadanense* from this study can be considered as the first record for Indian Ocean and extends the known range of geographical distribution for this species.

In the type locality, *P. sipadanense* has been rarely found among the epiphytic dinoflagellates occurring on seagrasses (Mohammad-Noor *et al*., 2007). Similarly, in this study the species was occasionally found associated with macroalgae in Oman. Based on known records, *P. sipadanense* appears to be rarely observed epiphytic species, and it may be restricted in distribution to tropical areas.

Acknowledgements

We acknowledge the help of Drs. Igor Polikarpov (Kuwait Institute for Scientific Research, Kuwait) and Mikhail Chesalin (Fisheries Research Center, Salalah, Oman) in

field sampling. The authors thank Dr. Normawaty Mohammad-Noor (International Islamic University, Malaysia) for providing high resolution images of the type material for *P. sipadanense* and Dr. Andrey Sazhin (P.P. Shirshov Institute of Oceanology, Moscow, Russia) for providing the optic facilities. We also acknowledge the help of Ms. Ahlam S. Al-Kadi and Mr. Mohammed T. Rajab (Nanoscopy Science Center, Kuwait University, Kuwait) and Mr. Viktor Karlov (P.P. Shirshov Institute of Oceanology, Moscow, Russia) for their skilful technical assistance with SEM. We are grateful to the associate editor Dr. Mona Hoppenrath and two anonymous reviewers for their detailed and constructive comments.

References

ALIGIZAKI, K., NIKOLAIDIS, G., KATIKOU, P., BAXEVANIS, A.D. & ABATZOPOULOS, T.J. (2009). Potentially toxic epiphytic *Prorocentrum* (Dinophyceae) species in Greek coastal waters. *Harmful Algae*, **8**: 299–311.

CHOMÉRAT, N. & COUTÉ, A. (2008). *Protoperidinium bolmonense* sp. nov. (Peridiniales, Dinophyceae), a small dinoflagellate from a brackish hypereutrophic lagoon (South of France). *Phycologia*, **47**~~(4)~~: 392–403.

FAUST, M.A. (1990). Morphologic details of six benthic species of *Prorocentrum* (Pyrrophyta) from a mangrove island, Twin Cays, Belize, including two new species. *Journal of Phycology*, **26**: 548–558.

FAUST, M.A. & GULLEDGE, R.A. (2002). Identifying harmful marine dinoflagellates. *Smithsonian Institution Contributions U.S. National Herbarium*, **42**: 1–144.

FAUST, M.A., LARSEN, J. & MOESTRUP, Ø. (1999). ICES identification leaflets for plankton. Leaflet no. 184. Potentially toxic phytoplankton. 3. Genus *Prorocentrum* (Dinophyceae). In *International Council for the Exploitation of the Sea*, Copenhagen, Denmark, 24 pp.

FAUST, M.A., LITAKER, R.W., VANDERSEA, M.W., KIBLER, S.R. & TESTER, P.A. (2005). Dinoflagellate diversity and abundance in two Belizean coral-reef mangrove lagoons: a test of Margalef's Mandala. *Atoll Research Bulletin*, **534**: 104–131.

FAUST, M.A., VANDERSEA, M.W., KIBLER, S.R., TESTER, P.A. & LITAKER, R.W. (2008). *Prorocentrum levis*, a new benthic species (Dinophyceae) from a mangrove island, Twin Cays, Belize. *Journal of Phycology*, **44**: 232–240.

FRITZ, L. & TRIEMER, R.E. (1985). A rapid simple technique utilizing calcofluor white MR2 for the visualization of dinoflagellate thecal plates. *Journal of Phycology*, **21**: 662–664.

GUINDON, S., DUFAYARD, J.-F., LEFORT, V., ANISIMOVA, M., HORDIJK, W. & GASCUEL, O. (2010). New algorithms and methods to estimate Maximum-Likelihood phylogenies: assessing the performance of PhyML 3.0. *Systematic Biology*, **59**: 307–321.

HERRERA-SEPÚLVEDA, A., MEDLIN, L.K., MURUGAN, G., SIERRA-BELTRÁN, A.P., CRUZ-VILLACORTA, A.A. & HERNÁNDEZ-SAAVEDRA, N.Y. (2015). Are *Prorocentrum hoffmannianum* and *Prorocentrum belizeanum* (Dinophyceae, Prorocentrales), the same species? An integration of morphological and molecular data. *Journal of Phycology*, **51**: 173–188.

HOPPENRATH, M., CHOMÉRAT, N., HORIGUCHI, T., SCHWEIKERT, M., NAGAHAMA, Y. & MURRAY S. (2013). Taxonomy and phylogeny of the benthic *Prorocentrum* species (Dinophyceae) - a proposal and review. *Harmful Algae*, **27**: 1–28.

HOPPENRATH, M., MURRAY, S., CHOMÉRAT, N., HORIGUCHI, T. (2014). *Marine benthic dinoflagellates - unveiling their worldwide biodiversity.* Kleine Senckenberg-Reihe, Band 54, Schweizerbart'sche Verlagbuchhandlung, Stuttgart.

KATOH, K. & STANDLEY, D.M. (2013). MAFFT multiple sequence alignment software version 7: improvements in performance and usability. *Molecular Biology and Evolution*, **30**: 772–780.

KELLER, M.D., SELVIN, R.C., CLAUS, W. & GUILLARD, R.R.L. (1987). Media for the culture of oceanic ultraphytoplankton. *Journal of Phycology*, **23**: 633–638.

LARSEN, J. & NGUYEN, N.L. (2004). Dinophyceae Pascher 1914. In *Potentially toxic microalgae of Vietnamese waters* (Larsen, J. & Nguyen, N.L., editors), *Opera Botanica*, **140**: 53–134.

MARANDA, L., CORWIN, S., DOVER, S. & MORTON, S.L. (2007). *Prorocentrum lima* (Dinophyceae) in northeastern USA coastal waters: II Toxin load in the epibiota and in shellfish. *Harmful Algae*, **6**~~(5)~~: 632–641.

MARASIGAN, A.N., TAMSE, A.F. & FUKUYO, Y. (2001). *Prorocentrum* (Prorocentrales: Dinophyceae) populations on seagrass-blade surface in Taklong Island, Guimaras Province, Philippines. *Plankton Biology and Ecology*, **48**~~(2)~~: 79–84.

MCNEILL, J., BARRIE, F.R., BURDET, H.M., DEMOULIN, V., HAWKSWORTH, D.L., MARHOLD, K., NICOLSON, D.H., PRADO, J., SILVA, P.C., SKOG, J.E., WIERSEMA, J.H. & TURLAND, N.J. (2006). *International Code of Botanical Nomenclature (Vienna Code)*. Regnum Vegetabile 146. A.R.G. Ganthner Verlag, KG.

MOESTRUP, Ø., AKSELMAN, R., CRONBERG, G., ELBRAECHTER, M., FRAGA, S., HALIM, Y., HANSEN, G., HOPPENRATH, M., LARSEN, J., LUNDHOLM, N., NGUYEN, L.N. & ZINGONE, A. (Eds) (2015). *IOC-UNESCO Taxonomic Reference List of Harmful Micro Algae* at http://www.marinespecies.org/hab/aphia.php?p=taxdetails&id =109566 on 2015-07-17.

MOHAMMAD-NOOR, N., DAUGBJERG, N., MOESTRUP, Ø. & ANTON, A. (2007). Marine epibenthic dinoflagellates from Malaysia – a study of live cultures and preserved samples based on light and scanning electron microscopy. *Nordic Journal of Botany*, **24**: 629–690.

NAGAHAMA, Y., MURRAY, S., TOMARU, A. & FUKUYO, Y. (2011). Species boundaries in the toxic dinoflagellate *Prorocentrum lima* (Dinophyceae, Prorocentrales), based on morphological and phylogenetic characters. *Journal of Phycology*, **47**: 178–189.

NÉZAN, E., TILLMANN, U., BILIEN, G.L., BOULBEN, S., CHÈZE, K., ZENTZ, F., SALAS, R. & CHOMÉRAT, N. (2012). Taxonomic revision of the dinoflagellate *Amphidoma caudata*: Transfer to the genus *Azadinium* (Dinophyceae) and proposal of two varieties, based on morphological and molecular phylogenetic analyses. *Journal of Phycology*, **48**: 925–939.

OKOLODKOV, Y.B., MERINO-VIRGILIO, F.C., AKÉ-CASTILLO, J.A., AGUILAR-TRUJILLO, A.C., ESPINOSA-MATÍAS, S. & HERRERA-SILVEIRA, J.A. (2014). Seasonal changes in epiphytic dinoflagellate assemblages near the northern coast of the Yucatan Peninsula, Gulf of Mexico. *Acta Botanica Mexicana*, **107**: 121–151.

POSADA, D. (2008). jModelTest: Phylogenetic model averaging. *Molecular Biology and Evolution*, **25**: 1253–1256.

PRUESSE, E., PEPLIES, J. & GLOCKNER, F.O. (2012). SINA: accurate high-throughput multiple sequence alignment of ribosomal RNA genes. *Bioinformatics*, **28**: 1823–1829.

RIXEN, T., HAAKE, B. & ITTEKKOT, V. (2000). Sedimentation in the western Arabian Sea: The role of coastal and open-ocean upwelling. In *Particle Flux and its preservation in Deep Sea Sediments* (Gansen, G. & Wefer, G., editors), *Deep-Sea Research II*, **47**: 2155–2178.

RONQUIST, F. & HUELSENBECK, J.P. (2003). MrBayes 3: Bayesian phylogenetic inference under mixed models. *Bioinformatics*, **19**: 1572–1574.

SABUROVA, M., AL-YAMANI, F. & POLIKARPOV, I. (2009). Biodiversity of free-living flagellates in Kuwait's intertidal sediments. In *Environment, Biodiversity and Conservation in the Middle East* (Krupp, F., Musselman, L.J., Kotb, M.M. A. & Weidig, I., editors), Proceedings of the First Middle Eastern Biodiversity Congress, Aqaba, Jordan, 20–23 October 2008, *Biorisk*, **3**: 97–110.

SHAH, M.M.R., AN, S.J. & LEE, J.B. (2013). Presence of benthic dinoflagellates around coastal waters of Jeju Island including newly recorded species. *Journal of Ecology and Environment*, **36**: 347–370.

STEIDINGER, K.A. & TANGEN, K. (1996). Dinoflagellates. In *Identifying Marine Phytoplankton* (Tomas, C.R., editor), 387–584, Academic Press, San Diego.

TEN-HAGE, L., TURQUET, J., QUOD, J.-P., PUISEUX-DAO, S. & COUTÉ, A. (2000). *Prorocentrum borbonicum* sp. nov. (Dinophyceae), a new toxic benthic dinoflagellate from the southwestern Indian Ocean. *Phycologia*, **39**: 296–301.

TEN-HAGE, L., ROBILLOT, C., TURQUET, J., LE GALL, F., LE CAER, J.-P., BULTEL, V., GUYOT, M. & MOLGÓ J. (2002). Effects of toxic extracts and purified borbotoxins

from *Prorocentrum borbonicum* (Dinophyceae) on vertebrate neuromuscular junctions. *Toxicon*, **40**: 137–148.

UHLIG, G. (1964). Eine einfache Methode zur Extraktion der vagilen mesopsammalen Mikrofauna. *Helgoländer Wissenschaftliche Meeresuntersuchungen*, **11**: 178–85.

Table 1. Comparison of morphometric (min-max [mean ± SD]) and morphological features in *P. sipadanense* and *P. borbonicum*

	*Prorocentrum sipadanense**	*Prorocentrum sipadanense***	*Prorocentrum borbonicum****
Cell length, µm	17.9-23.9 [21.90 ± 1.22]	18-19	18-24 [20.0 ± 1.2]
Cell width, µm	15.7-19.8 [18.16 ± 0.87]	15-16	14-20 [18.0 ± 1.0]
Length/Width ratio	1.13-1.45 [1.22 ± 0.06]	1.19[a]	1.11[a]
Cell shape	Ovoid	Round to oval	Broad oval to ovoid
Asymmetry of apex[b]	Oblique truncated	Slightly oblique truncated[c]	Truncated
Dorsal apical edge	Lower and truncated	Slightly lower and truncated[c]	Truncated
Ventral apical edge	Higher and pointed	Slightly higher and pointed[c]	Pointed
Marginal ridge	prominent	prominent[c]	No
Periflagellar area	Oblique, wide V-shaped	Slightly oblique, wide V-shaped	Wide V-shaped
No. of platelets	9 (1 2 3 4 5 6a 6b 7 8 9)	8? (1 2 3 4 5 6 7 8)	8-9 (1 2 3 4 5 6a 6b 7 8 9)
Flagellar pore	Yes	Yes	Yes
Accessory pore	Yes	?	Yes
Apical indention	RV	RV	RV, LV

Theca ornamentation	Foveate to reticulate	Foveate	Foveate
Depression size	0.24-0.75 [0.59±0.15]	0.26-0.45[d]	0.4-0.5
Pore size	Large: No	Large: No	Large - 0.16-0.17
	Small: 0.11-0.18 [0.14 ± 0.02]	Small: 0.11-0.16[d]	Small - 0.07-0.08
Pore pattern	Distinct (pair/triplet/single pores)	Distinct	Scattered
Plate centre	Devoid of pores	Devoid of pores	Devoid of large pores, with small pores
Position of pores	In depressions	In depressions	In depressions and between
Marginal pores	Yes	Yes	No
No. of ~~valve~~thecal pores	20-26	14[d]	c.a. 80 (LV)-100 (RV)[d]
No. of marginal pores	39-47	27-28[d]	No
Intercalary band	Smooth	Striated ?[e]	Smooth (outer)/Striated (inner)
Pyrenoid	Yes	?	Yes
Nucleus	Small, posterior	?	Small, posterior

* - this study; ** - original description (Mohammad-Noor *et al*., 2007); *** - Ten-Hage *et al*., 2000; 2002; [a] – as calculated from published data; [b] - in right thecal view; [c] – omitted in original description but visible in provided illustrations; [d] – as calculated from provided illustrations; [e] – described as striated but appears to be smooth in provided illustrations.

Figure legends

Figs 1–13. Light micrographs of *Prorocentrum sipadanense*. **Figs 1-4**. Right lateral view of living cells in different focal planes showing the foveate thecal surface, the marginal ridge around cell, oblique truncated apex, centrally located pyrenoid (arrow), apically located pusule (p) and posteriorly located nucleus (n). **Figs 5, 6**. Left lateral view of living cells with centrally located pyrenoid (arrow) and posterior nucleus (n) visible. **Fig. 7**. Cell in lateral ~~valve~~thecal plate view under blue-light-excitation showing chlorophyll fluorescence of reticulate chloroplast with centrally located pyrenoid. **Fig. 8**. Cell in ~~ventral~~intercalary band view under blue-light-excitation showing two chloroplast lying along each ~~valve~~thecal plate (arrows). **Figs 9, 10**. Living cell in apical view in different focal planes with pusule (p) and two pyrenoids (arrows) visible. **Fig. 11**. Living cell in antapical view with nucleus (n) visible. **Fig. 12**. Empty theca in oblique right lateral view showing the foveate thecal surface, the marginal ridge around cell and pore pattern. **Fig. 13**. Empty theca in oblique ~~ventral~~intercalary band view with marginal pores and ridge visible. Scale bars: 5 µm.

Figs 14–20. Light micrographs of *Prorocentrum sipadanense* cells stained with Calcofluor White. **Fig. 14**. Right lateral view showing the cell outline. **Figs 15, 16**. Cells in right lateral view in high focal plane showing the foveate thecal surface and ~~valve~~thecal pores arrangement. **Fig. 17**. Flattened theca in right lateral view showing periflagellar area position (pa), intercalary band (ib) and pore pattern: pairs (2), triplets (3) and single (1) ~~valve~~thecal pores and uneven row of marginal pores (mp). **Fig. 18**. Split theca in antapical view with foveate surface, intercalary band and marginal pores visible. **Fig. 19**. Split theca in apical view showing the periflagellar area structure. **Fig. 20**. Detail of apical view in split theca showing the periflagellar~~e~~ area composition: large flagellar pore (fp), small accessory pore (as) and nine platelets (1, 2, 3, 4, 5, 6a, 6b, 7, 8). Scale bars: 5 µm.

Figs 21–27. SEM micrographs of *Prorocentrum sipadanense*. **Fig. 21**. Right lateral view. **Fig. 22**. Apical view. **Figs 23, 24**. Detail of apical end showing the periflagellar area. **Fig. 25**. Left lateral view. **Fig. 26**. Detail of thecal surface showing central area devoid of pores, ~~valve~~thecal pores (black arrows) and irregular row of marginal pores (white arrows). **Fig. 27**. Aggregated cells in culture. Scale bars: 2 µm in Figs 23, 24 and 26; 5 µm in Figs 21, 22 and 25; 10 µm in Fig. 27.

Figs 28–30. Light micrographs of *Prorocentrum sipadanense*. **Fig. 28**. Different cell morphotypes in culture with one motile cell and two nonmotile cells that embedded in chains of their nested half-open empty thecae visible; note the difference in size between morphotypes. **Figs 29, 30**. Small nonmotile cells in old culture embedded in chains of their nested half-open empty thecae. Scale bars: 10 µm.

Fig. 31. Maximum likelihood (ML) phylogenetic tree inferred from SSU rDNA (matrix of 38 taxa and 1719 aligned positions). Model selected GTR + I + Γ_4. Log likelihood = -7292.36 Substitution rate matrix: A ↔ C = 1.34307, A ↔ G = 4.06337, A ↔ T = 1.16826, C ↔ G = 0.56267, C ↔ T = 9.05979, against G ↔ T = 1.00000. Assumed nucleotide frequencies: f(A)=0.26207, f(C)=0.20011, f(G)=0.26363, f(T)=0.27420. Among site rate variation: assumed proportion of invariable sites I = 0.510. Rates at variable site assumed to be gamma distributed with shape parameter α = 0.692. Bootstrap values (1,000 pseudoreplicates) > 65 (in ML) and posterior probabilities > 0.5 (in BI) are shown at nodes, thick lines indicate full support of the branch (100/1.00). '+' indicate nodes present but unsupported.

Fig. 32. Maximum likelihood (ML) phylogenetic tree inferred from LSU rDNA (matrix of 34 taxa and 955 aligned positions). Model selected GTR + I + Γ_4. Log likelihood = -10816.46

Substitution rate matrix: A ↔ C = 0.67254, A ↔ G = 1.37936, A ↔ T = 0.48125, C ↔ G = 0.79139, C ↔ T = 4.04383, against G ↔ T = 1.00000. Assumed nucleotide frequencies: f(A)=0.25072, f(C)=0.20921, f(G)=0.30459, f(T)=0.23548. Among site rate variation: assumed proportion of invariable sites I = 0.149. Rates at variable site assumed to be gamma distributed with shape parameter α = 0.686. Bootstrap values (1,000 pseudoreplicates) > 65 (in ML) and posterior probabilities > 0.5 (in BI) are shown at nodes, thick lines indicate full support of the branch (100/1.00). '+' indicate nodes present but unsupported.

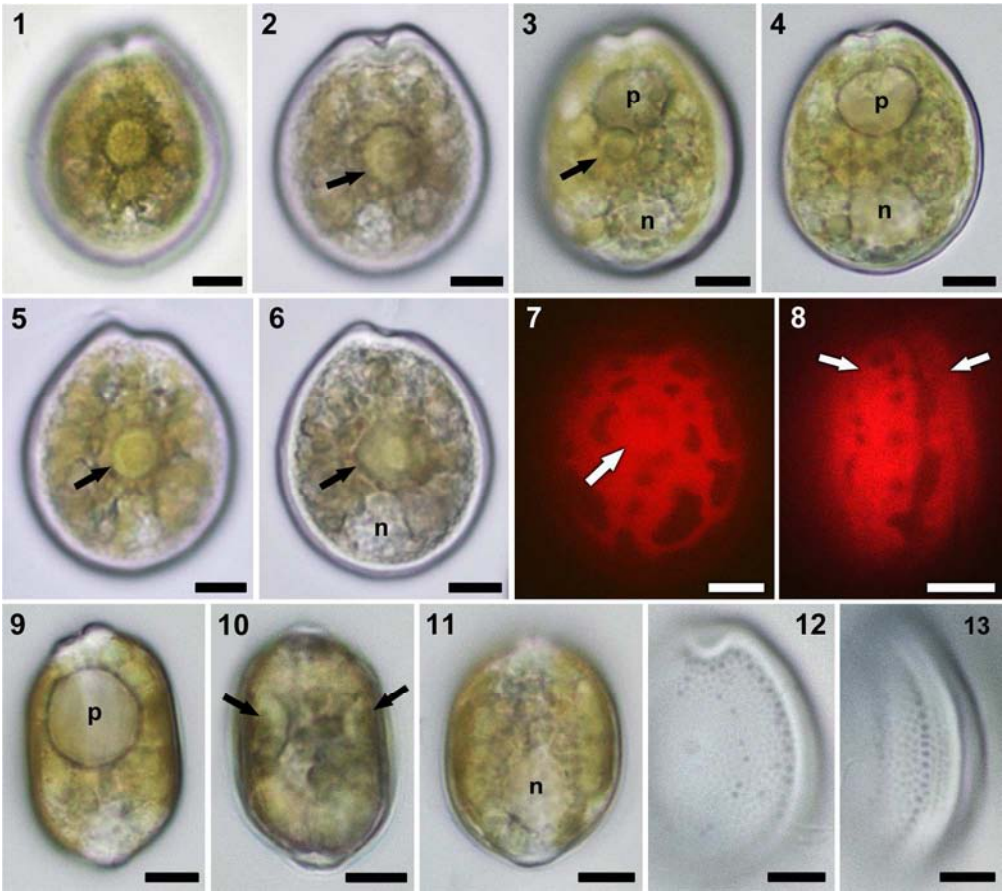

Figs 1–13. Light micrographs of Prorocentrum sipadanense. Figs 1-4. Right lateral view of living cells in different focal planes showing the foveate thecal surface, the marginal ridge around cell, oblique truncated apex, centrally located pyrenoid (arrow), apically located pusule (p) and posteriorly located nucleus (n). Figs 5, 6. Left lateral view of living cells with centrally located pyrenoid (arrow) and posterior nucleus (n) visible. Fig. 7. Cell in lateral thecal plate view under blue-light-excitation showing chlorophyll fluorescence of reticulate chloroplast with centrally located pyrenoid. Fig. 8. Cell in intercalary band view under blue-light-excitation showing two chloroplast lying along each thecal plate (arrows). Figs 9, 10. Living cell in apical view in different focal planes with pusule (p) and two pyrenoids (arrows) visible. Fig. 11. Living cell in antapical view with nucleus (n) visible. Fig. 12. Empty theca in oblique right lateral view showing the foveate thecal surface, the marginal ridge around cell and pore pattern. Fig. 13. Empty theca in oblique intercalary band view with marginal pores and ridge visible. Scale bars: 5 µm.
170x150mm (300 x 300 DPI)

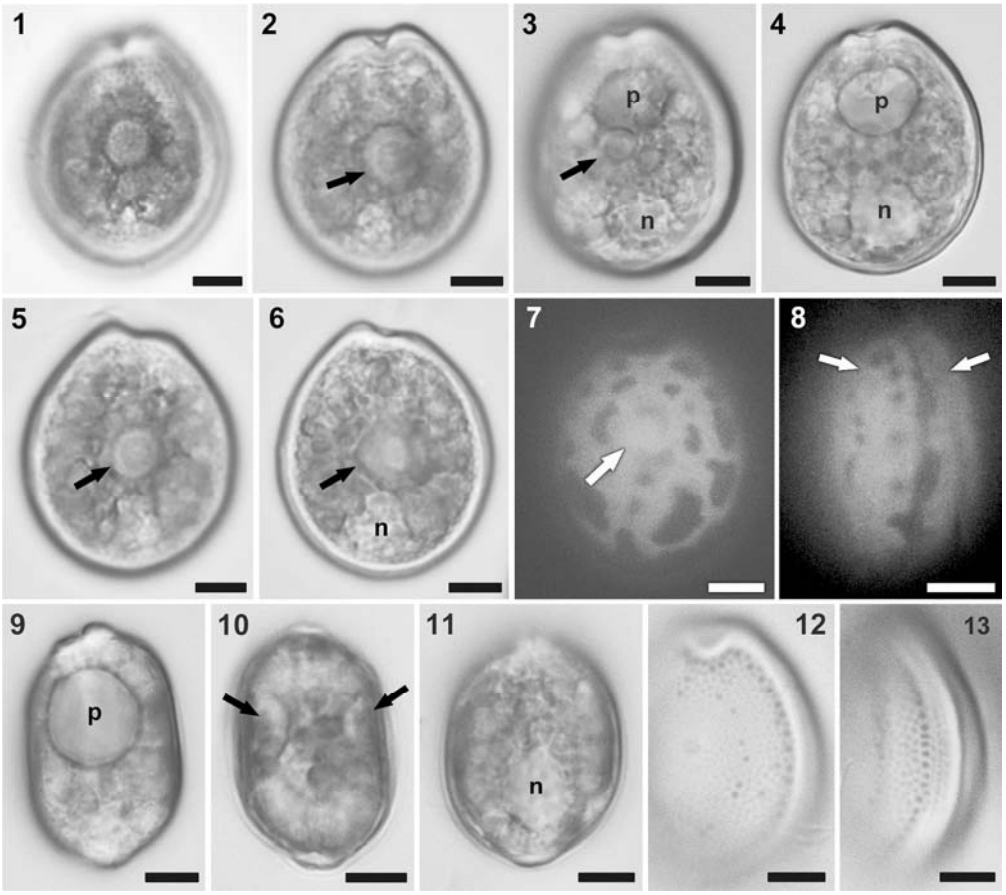

Figs 1–13. Light micrographs of Prorocentrum sipadanense. Figs 1-4. Right lateral view of living cells in different focal planes showing the foveate thecal surface, the marginal ridge around cell, oblique truncated apex, centrally located pyrenoid (arrow), apically located pusule (p) and posteriorly located nucleus (n). Figs 5, 6. Left lateral view of living cells with centrally located pyrenoid (arrow) and posterior nucleus (n) visible. Fig. 7. Cell in lateral thecal plate view under blue-light-excitation showing chlorophyll fluorescence of reticulate chloroplast with centrally located pyrenoid. Fig. 8. Cell in intercalary band view under blue-light-excitation showing two chloroplast lying along each thecal plate (arrows). Figs 9, 10. Living cell in apical view in different focal planes with pusule (p) and two pyrenoids (arrows) visible. Fig. 11. Living cell in antapical view with nucleus (n) visible. Fig. 12. Empty theca in oblique right lateral view showing the foveate thecal surface, the marginal ridge around cell and pore pattern. Fig. 13. Empty theca in oblique intercalary band view with marginal pores and ridge visible. Scale bars: 5 µm.
170x150mm (300 x 300 DPI)

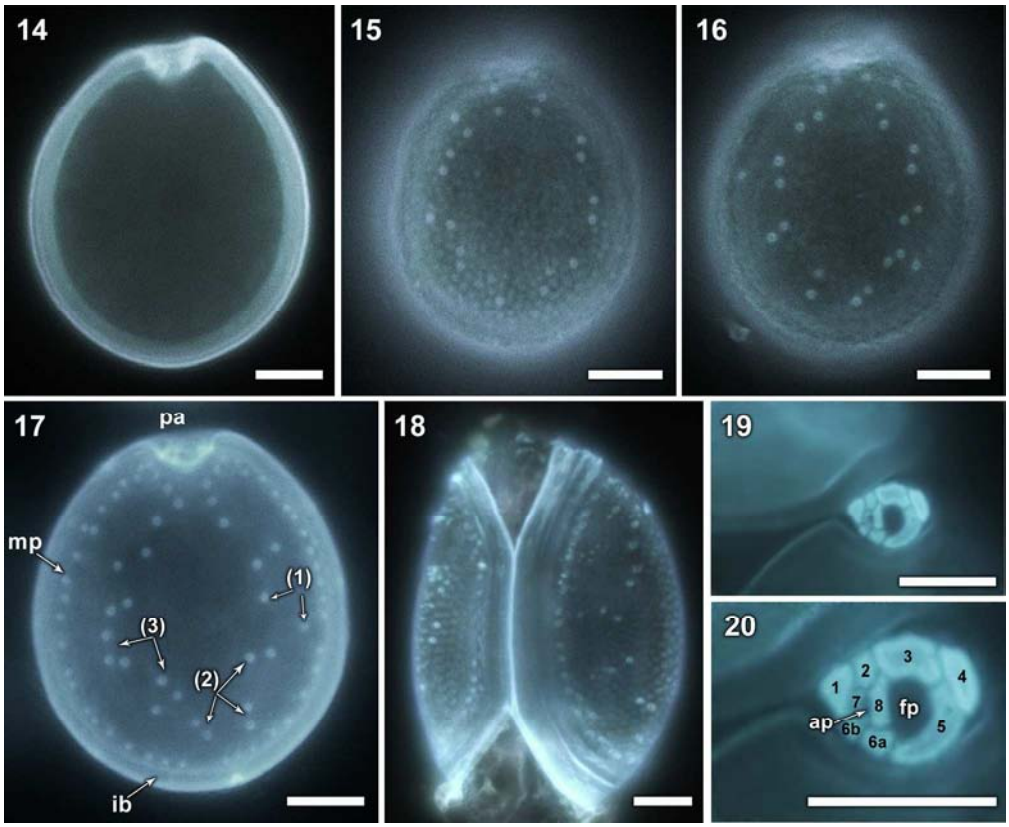

Figs 14–20. Light micrographs of Prorocentrum sipadanense cells stained with Calcofluor White. Fig. 14. Right lateral view showing the cell outline. Figs 15, 16. Cells in right lateral view in high focal plane showing the foveate thecal surface and thecal pores arrangement. Fig. 17. Flattened theca in right lateral view showing periflagellar area position (pa), intercalary band (ib) and pore pattern: pairs (2), triplets (3) and single (1) thecal pores and uneven row of marginal pores (mp). Fig. 18. Split theca in antapical view with foveate surface, intercalary band and marginal pores visible. Fig. 19. Split theca in apical view showing the periflagellar area structure. Fig. 20. Detail of apical view in split theca showing the periflagellar area composition: large flagellar pore (fp), small accessory pore (as) and nine platelets (1, 2, 3, 4, 5, 6a, 6b, 7, 8). Scale bars: 5 µm.
170x138mm (300 x 300 DPI)

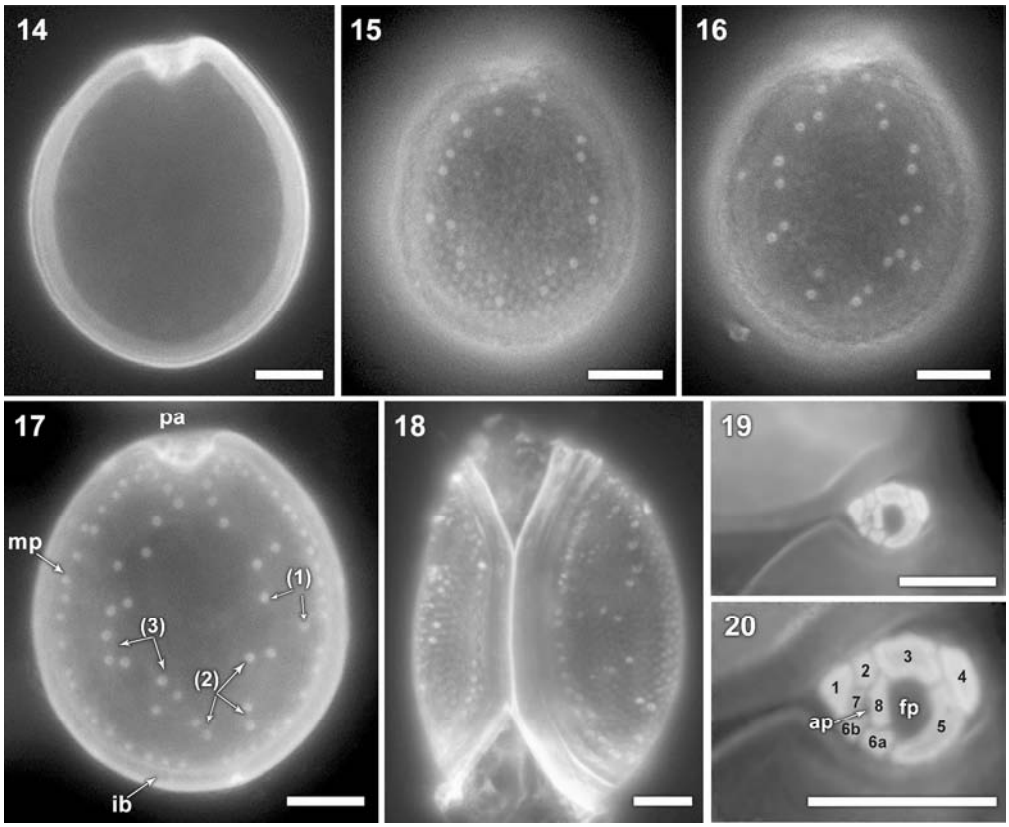

Figs 14–20. Light micrographs of Prorocentrum sipadanense cells stained with Calcofluor White. Fig. 14. Right lateral view showing the cell outline. Figs 15, 16. Cells in right lateral view in high focal plane showing the foveate thecal surface and thecal pores arrangement. Fig. 17. Flattened theca in right lateral view showing periflagellar area position (pa), intercalary band (ib) and pore pattern: pairs (2), triplets (3) and single (1) thecal pores and uneven row of marginal pores (mp). Fig. 18. Split theca in antapical view with foveate surface, intercalary band and marginal pores visible. Fig. 19. Split theca in apical view showing the periflagellar area structure. Fig. 20. Detail of apical view in split theca showing the periflagellar area composition: large flagellar pore (fp), small accessory pore (as) and nine platelets (1, 2, 3, 4, 5, 6a, 6b, 7, 8). Scale bars: 5 µm.
170x138mm (300 x 300 DPI)

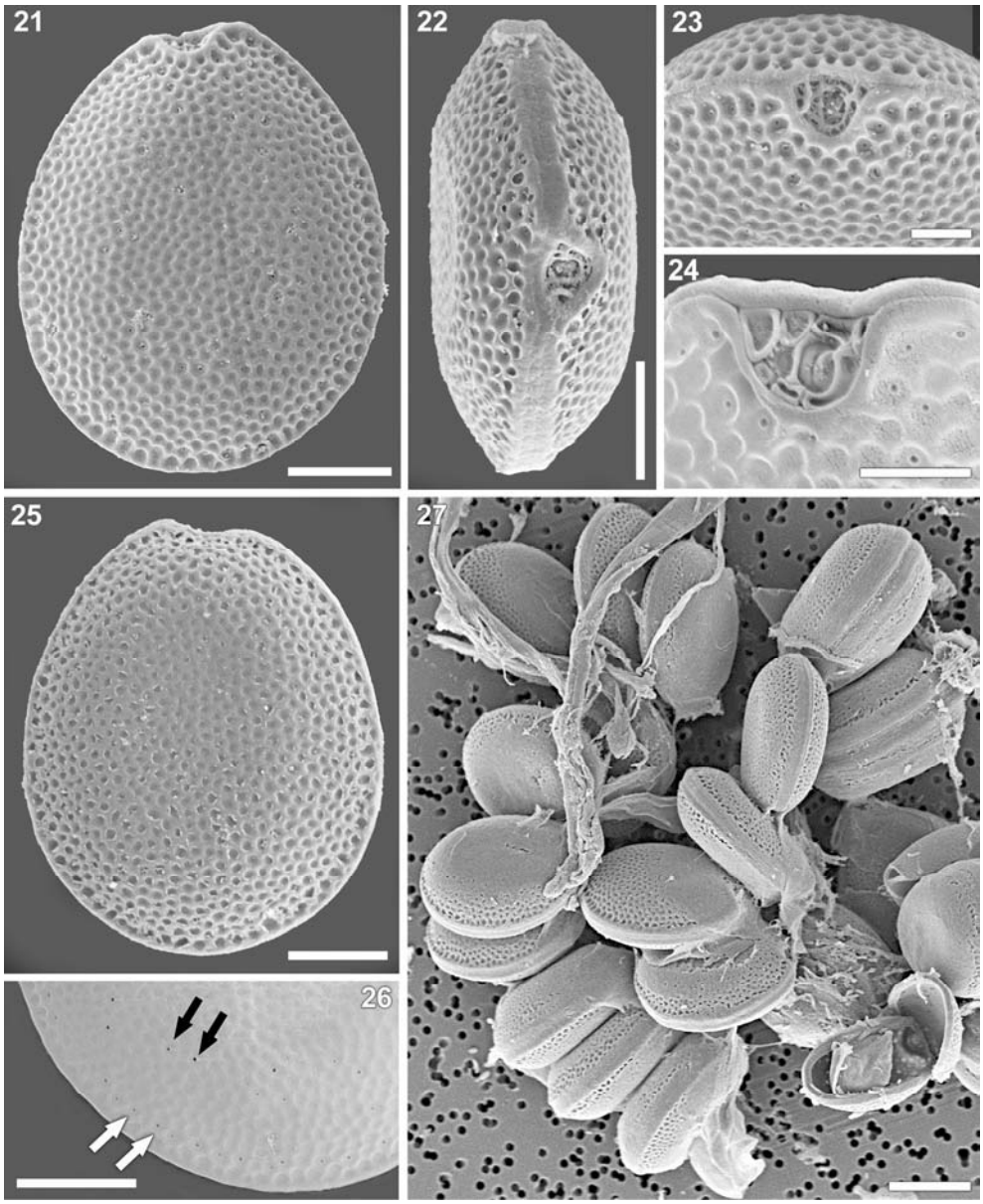

Figs 21–27. SEM micrographs of Prorocentrum sipadanense. Fig. 21. Right lateral view. Fig. 22. Apical view. Figs 23, 24. Detail of apical end showing the periflagellar area. Fig. 25. Left lateral view. Fig. 26. Detail of thecal surface showing central area devoid of pores, thecal pores (black arrows) and irregular row of marginal pores (white arrows). Fig. 27. Aggregated cells in culture. Scale bars: 2 µm in Figs 23, 24 and 26; 5 µm in Figs 21, 22 and 25; 10 µm in Fig. 27.
170x207mm (300 x 300 DPI)

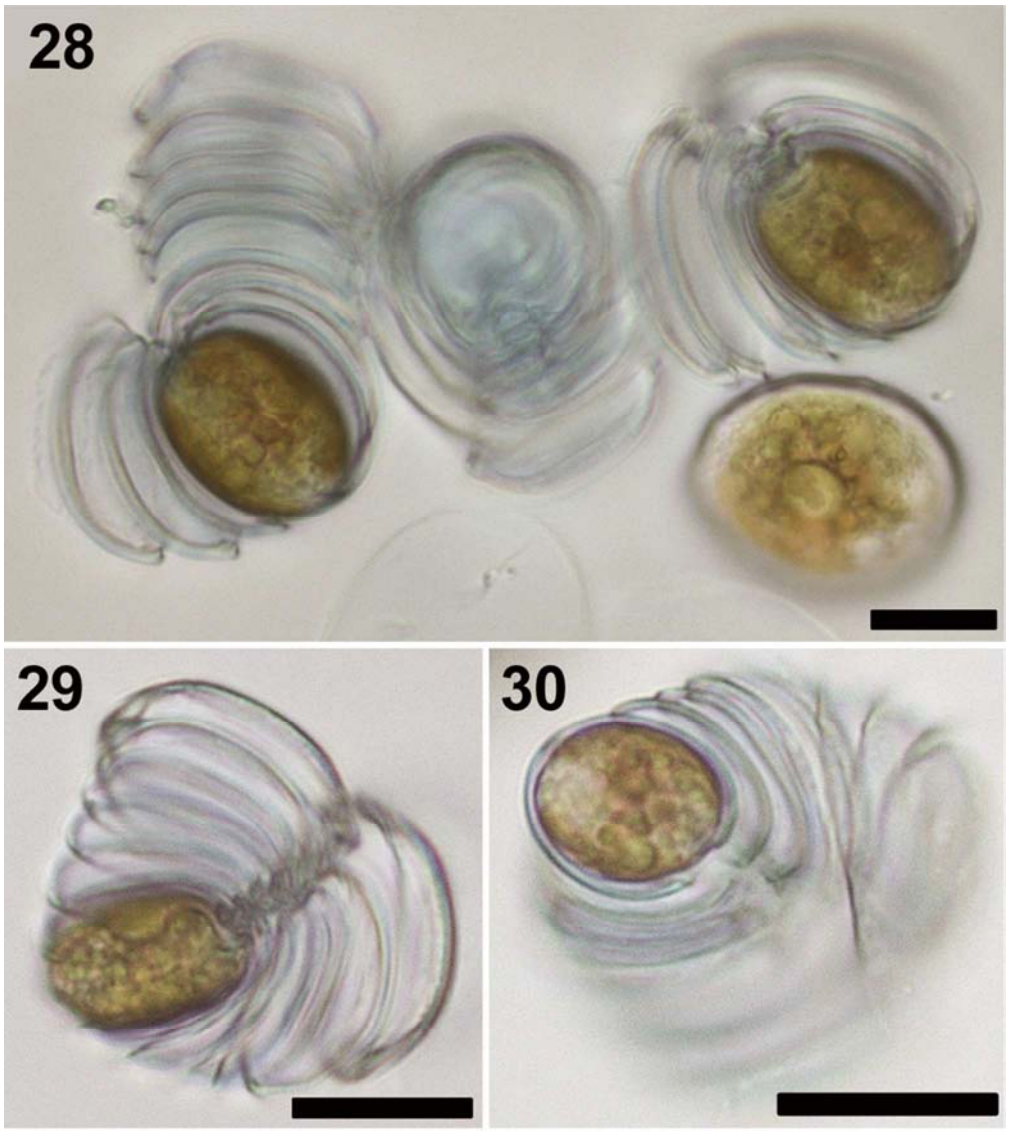

Figs 28–30. Light micrographs of Prorocentrum sipadanense. Fig. 28. Different cell morphotypes in culture with one motile cell and two nonmotile cells that embedded in chains of their nested half-open empty thecae visible; note the difference in size between morphotypes. Figs 29, 30. Small nonmotile cells in old culture embedded in chains of their nested half-open empty thecae. Scale bars: 10 μm.
80x89mm (300 x 300 DPI)

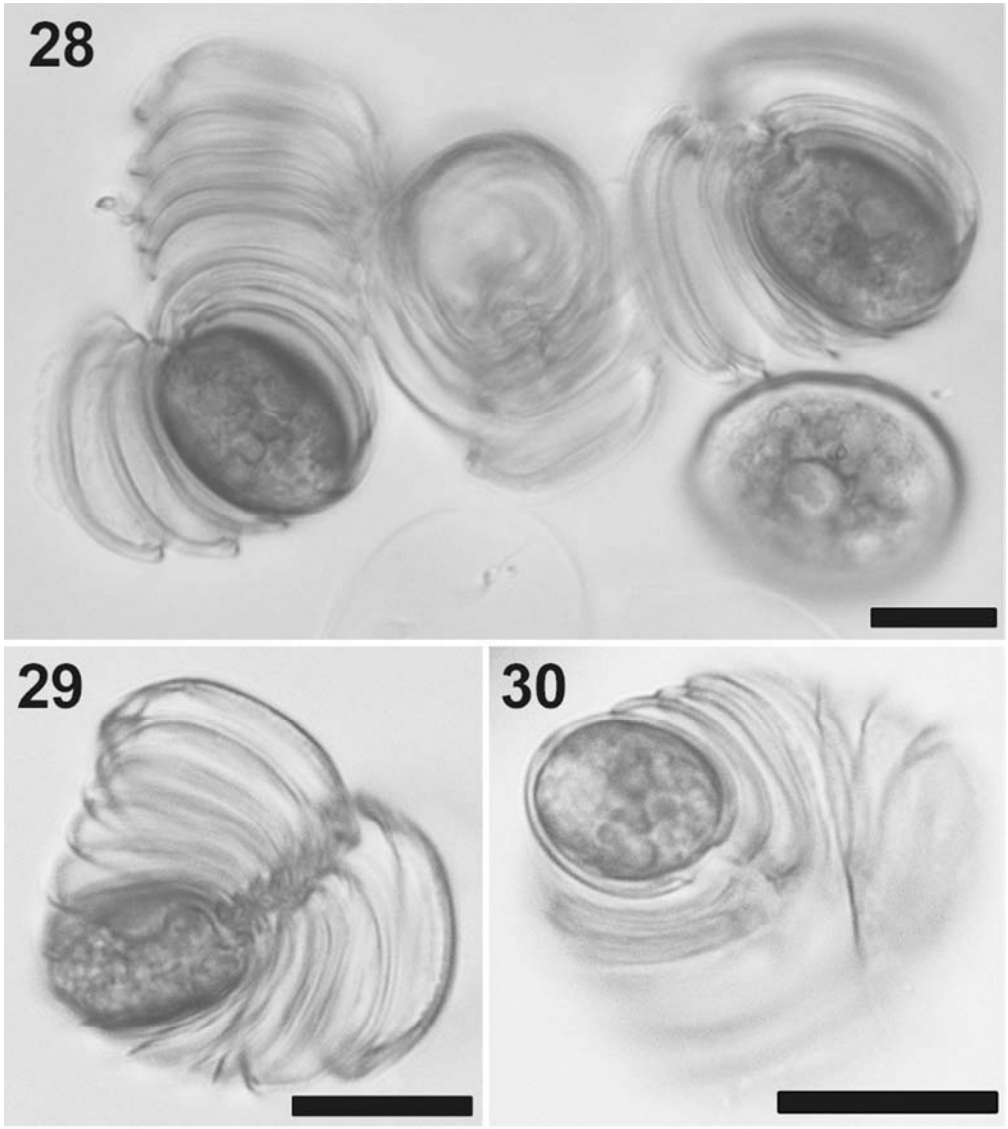

Figs 28–30. Light micrographs of Prorocentrum sipadanense. Fig. 28. Different cell morphotypes in culture with one motile cell and two nonmotile cells that embedded in chains of their nested half-open empty thecae visible; note the difference in size between morphotypes. Figs 29, 30. Small nonmotile cells in old culture embedded in chains of their nested half-open empty thecae. Scale bars: 10 μm.
80x89mm (300 x 300 DPI)

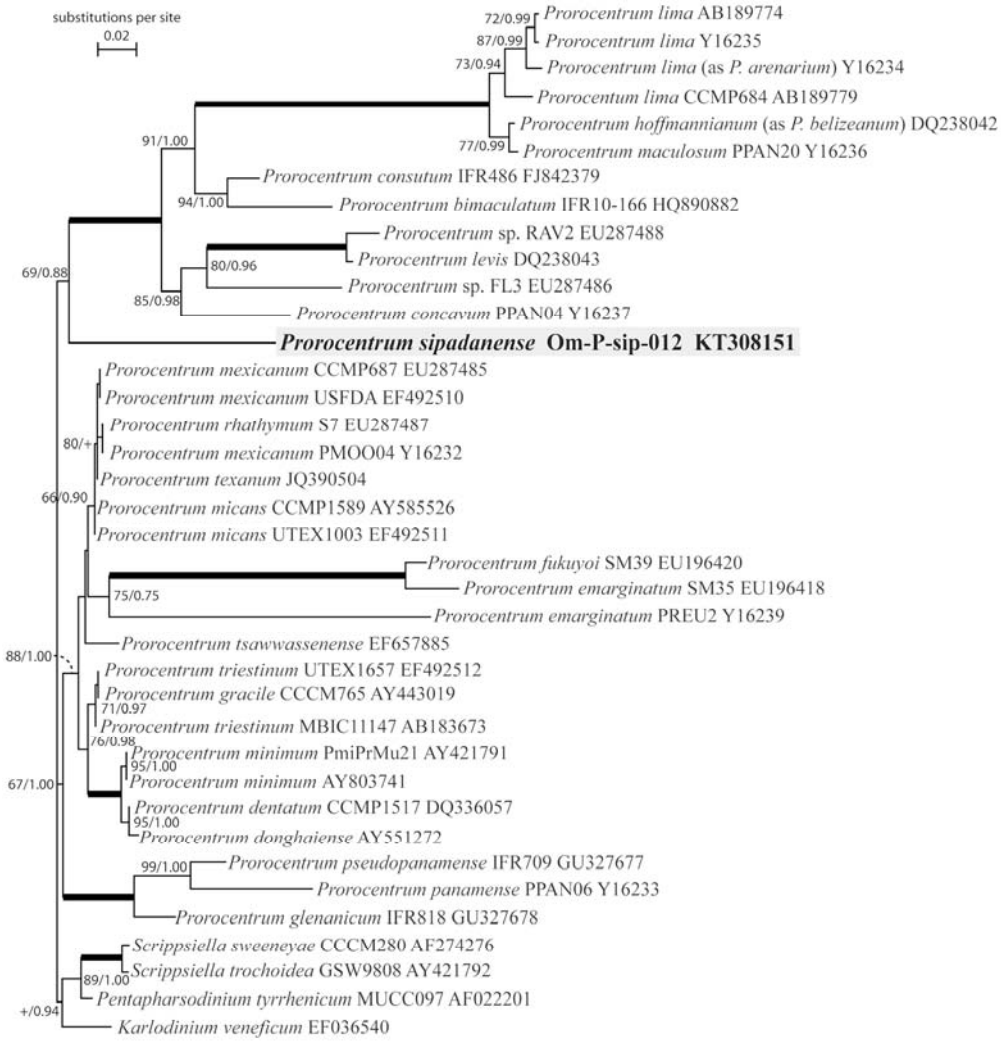

Fig. 31. Maximum likelihood (ML) phylogenetic tree inferred from SSU rDNA (matrix of 38 taxa and 1719 aligned positions). Model selected GTR + I + Γ4. Log likelihood = 7292.36 Substitution rate matrix: A ↔ C = 1.34307, A ↔ G = 4.06337, A ↔ T = 1.16826, C ↔ G = 0.56267, C ↔ T = 9.05979, against G ↔ T = 1.00000. Assumed nucleotide frequencies: f(A)=0.26207, f(C)=0.20011, f(G)=0.26363, f(T)=0.27420. Among site rate variation: assumed proportion of invariable sites I = 0.510. Rates at variable site assumed to be gamma distributed with shape parameter α = 0.692. Bootstrap values (1,000 pseudoreplicates) > 65 (in ML) and posterior probabilities > 0.5 (in BI) are shown at nodes, thick lines indicate full support of the branch (100/1.00). '+' indicate nodes present but unsupported.
170x178mm (300 x 300 DPI)

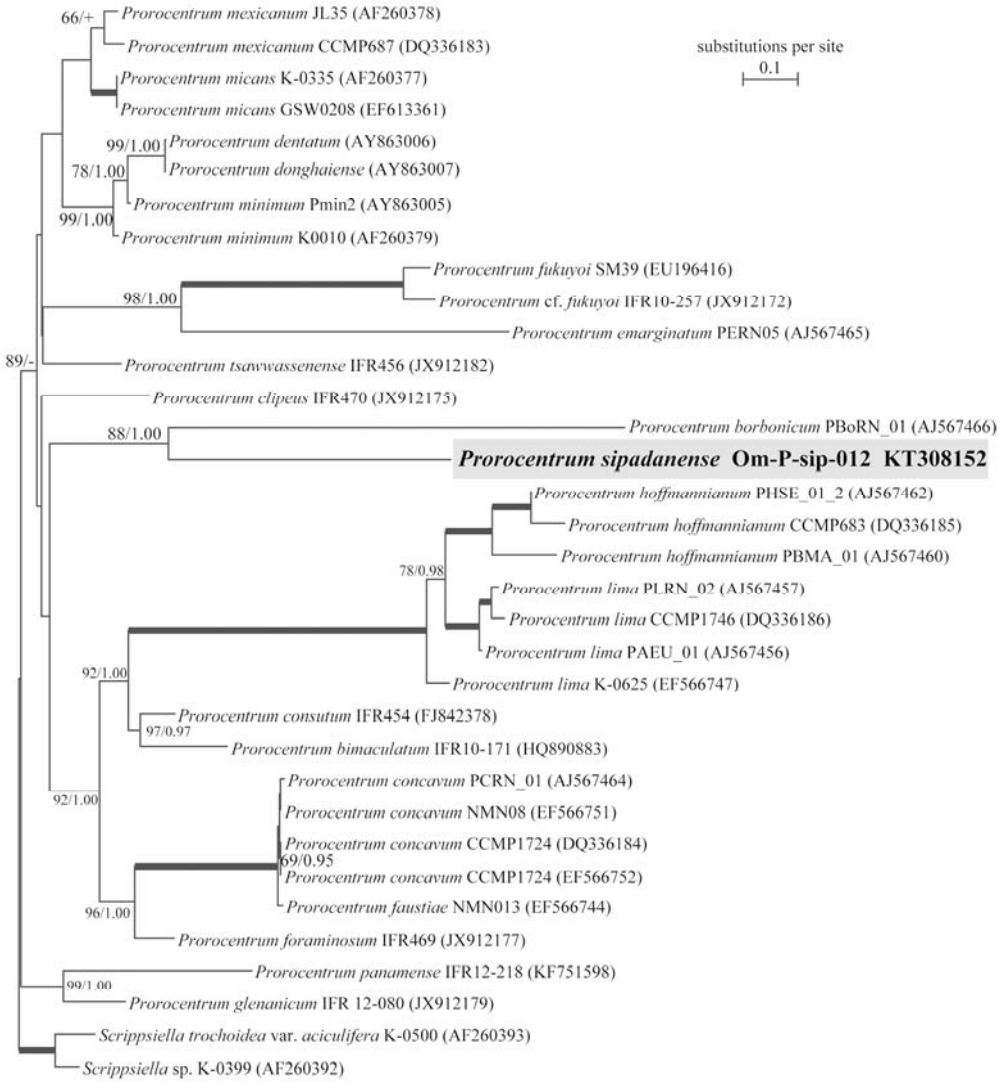

Fig. 32. Maximum likelihood (ML) phylogenetic tree inferred from LSU rDNA (matrix of 34 taxa and 955 aligned positions). Model selected GTR + I + Γ4. Log likelihood = 10816.46 Substitution rate matrix: A ↔ C = 0.67254, A ↔ G = 1.37936, A ↔ T = 0.48125, C ↔ G = 0.79139, C ↔ T = 4.04383, against G ↔ T = 1.00000. Assumed nucleotide frequencies: f(A)=0.25072, f(C)=0.20921, f(G)=0.30459, f(T)=0.23548. Among site rate variation: assumed proportion of invariable sites I = 0.149. Rates at variable site assumed to be gamma distributed with shape parameter α = 0.686. Bootstrap values (1,000 pseudoreplicates) > 65 (in ML) and posterior probabilities > 0.5 (in BI) are shown at nodes, thick lines indicate full support of the branch (100/1.00). '+' indicate nodes present but unsupported.
170x184mm (300 x 300 DPI)